

# INTRODUCTION OF SEPARATION BOUNDARY IN SUB-PIXEL MAPPING BASED ON ATTRACTION MODEL

Armin Eskandari Nasab<sup>1</sup>, Azam Karami<sup>1,2</sup>, Sayyed Ashkan Adibi<sup>1</sup>

<sup>1</sup>Faculty of Physics, Shahid Bahonar University of Kerman, Kerman, Iran

<sup>2</sup>iMinds- Visionlab, University of Antwerp, Belgium

## ABSTRACT

In this paper, a new sub-pixel mapping method is proposed. This method uses sub-pixel spatial attraction model in order to separate existing endmembers in the mixed pixels. Each endmember is attracted by similar endmember in neighboring pixels and repulsed by the others. After that, a specific shape for each endmember is considered. This shape depends on the number of endmembers and their abundance fractions in the mixed pixels. This method is compared with sub-pixel spatial attraction model (SPSAM) and efficiency of our algorithm is shown by calculating the classification accuracy. Proposed algorithm could be significantly increased the classification accuracy.

**Index Terms**— sub-pixel, hard classification, attraction, mixed pixels

## 1. INTRODUCTION

Recently, hyperspectral images (HSI) have been used in many practical applications such as agriculture, defense, geology and etc. Some hyperspectral sensors usually have high spatial and low spectral resolutions such as AVIRIS<sup>1</sup> and Hyperion<sup>2</sup>. In real applications, low spatial resolution causes mixed pixels and decreases the classification accuracy. In fact, the mixed pixels are contained different endmembers. Our aim is to divide the mixed pixels into pure sub-pixels. Recently different methods for sub-pixel mapping such as fusing a high spatial resolution image (e.g. multispectral or panchromatic) with HSI [1][2][3], linear optimization [4], Hopfield neural network [5][6], pixel swapping [7] and sub-pixel spatial attraction model [8] are introduced. In [9], increasing the spatial resolution of HSI is considered as a post-processing step. In [8] a method based on sub-pixel/pixel attraction models (SPSAM) has been introduced which divides each pixel into some sub-pixels. The number of sub-pixel for each endmember depends on its abundance fraction value. This method calculates the attraction between each sub-pixel and neighboring pixels for all endmembers. Each endmember locates at sub-pixels where the attraction for that endmember is the highest.

Another method in [10] considers not only the attraction but also the repulsion too. Attraction and repulsion is calculated between sub-pixels of neighboring pixels and sub-pixels of central pixel. Using pixel swapping method which introduced in [7] the best location for each endmember is defined which attraction has the maximum value and repulsion has the minimum value. In this paper, a new non-iterative method for sub-pixel mapping based on attraction model is presented. The proposed method includes two main parts. First, a point for each endmember is introduced which gathers all sub-pixels with the same endmember and is called collection point (CP). Unlike the existing methods which calculate attraction or repulsion for all subpixels of the initial pixel, this method calculates attraction and repulsion only for a CP. This point is attracted by same neighboring pixel endmember and repulsed by the others. After applying attractions and repulsions, the CPs are located at the margin of the initial pixel. Second, a specific boundary is introduced for each endmember in order to separate every endmember from the others which is called Separation Boundary (SB). In other words, SB divides a pixel into pure sub-pixels and each pure pixel is related to a specific endmember. Depending on abundance fraction values, the sub-pixel area for different endmember existing in a mixed pixel can be equal or unequal. The shape of SB depends on the number endmembers. As an example, for mixed pixels with two endmembers, SB is a straight line and for more than two endmembers, it is like a curve. Finally, sub-pixels are collected around the CP and between pixel margin and SB. The rest of the paper is organized as follows. In Section 2, proposed method is described. Section 3 presents the experimental results and Section 4 concludes the paper.

## 2. PROPOSED METHOD

Proposed method includes four main steps as follow :

1) Each mixed pixel is divided into  $S \times S$  sub-pixels. The initial image has a low resolution as  $R_i$  and the final image has a high resolution as  $R_f$ .  $R_i = M \times N$  and  $R_f = SM \times SN$  where  $M$  and  $N$  are the number of row and column of the initial image respectively and  $S$  is the scaling factor. The number of sub-pixels for each endmember depends on its abundance fraction value.

<sup>1</sup><http://aviris.jpl.nasa.gov/index>

<sup>2</sup><https://eo1.usgs.gov/sensors/hyperion>

2) Each endmember is collected around a CP is nominated by  $C_i$  where  $C_i$  is a point and  $i$  refers to each existing endmember in the initial pixel. In order to find the best position of  $C_i$ , it is assumed that  $C_i$  is similar to a floating object at the center of the initial pixel which could be attracted by the same endmember and repulsed by the other existing endmembers existed in neighboring pixels. Attraction and repulsion are shown by a binding force  $F_i$  which is expressed as follow:

$$F_i = \sum_{j=1}^8 \sum_{k=1}^N \frac{\alpha_k A_{jk}}{r_j^2} \quad (1)$$

where  $j = 1, 2, \dots, 8$  and  $j$  shows neighboring pixels;  $k = 1, 2, \dots, N$  where  $N$  is the number of endmembers in  $j$ th neighbor;  $A_{jk}$  is abundance fraction of  $k$ th endmember in  $j$ th neighboring pixel; This force is an attraction force when  $\alpha_k$  is equal to 1 and it is a repulsion force when  $\alpha_k$  equals to -1;  $r_j$  is the Euclidean distance between the center of initial pixel and the center of the  $j$ th neighbor. In this case,  $C_i$  is pulled by  $F_i$  toward the margin of the initial pixel. The location of  $C_i$  is updated at the margin of the initial pixel. Sub-pixels with  $i$ th endmember should collect around the  $C_i$ . Each endmember is separated from other endmembers with a SB.

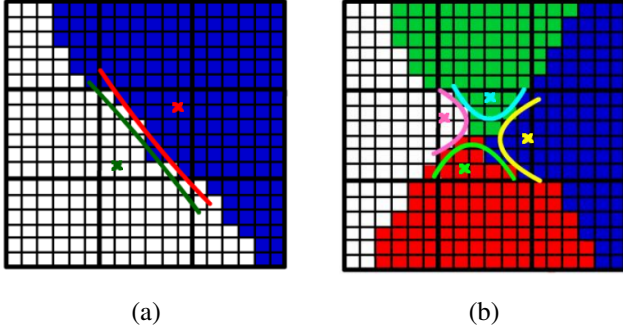


**Fig. 1.** Different shape of SB. (a) 2 endmembers (b) 4 endmembers

3) As shown in Fig. 1 each endmember is separated by a boundary which is called Separation Boundary (SB). In fact, in all situations, SB is part of the boundary of a hypothetical circle which is called  $Cr_i$ . In this step  $Cr_i$  crosses the  $C_i$  and its center is located out of the initial pixel. The resulting vector between center of  $Cr_i$  and  $C_i$  has same direction as  $F_i$ .  $Cr_i$  in pixels with fewer endmembers has a bigger radius. Thus the radius of  $Cr_i$  varies with  $N$  inversly which is shown in the following equation:

$$L_i = a \times \left(\frac{1}{N}\right)^b \quad (2)$$

where  $L_i$  is the initial radius of the  $Cr_i$ ;  $a$  and  $b$  are constants and should be set. Approximately in mixed pixels with

2 or 3 endmembers  $L_i$  should have a large value and in the mixed pixel with 5, 6 or more endmembers  $L_i$  should have a small value. After examining of different values, following experimental formula are suggested:

$$a = 5 \times 10^3$$

$$b = 5$$

However the proposed algorithm is not very sensitive to  $a$  and  $b$  values. Any desired values for  $a$  and  $b$  with the mentioned orders can be used.

4) SB divides the initial pixel into different areas which each endmember located inside one part. Thus,  $Cr_i$  should not cross the  $C_i$ . SB must cross a point inside the initial pixel but not the center of it necessarily. Because if SB cross the center of the initial pixel, each pixel is divided into equal parts and it is obvious in most of the mixed pixels the abundance fraction value of different endmembers are not the same. In fact SB crosses the weighted average position ( $AP$ ) of all  $C_i$  which is and it is expressed as follows:

$$AP = \frac{\sum_{i=1}^N (1 - W_i) C_i}{\sum_{i=1}^N W_i} \quad (3)$$

where  $W_i$  is abundance fraction of endmember  $i$  and has a value between 0 and 1. After  $AP$  is calculated, the Euclidean distance between  $AP$  and  $C_i$  is calculated and expressed as  $d_i$  and then it is added to  $L_i$ . The final radius of  $Cr_i$  is expressed as  $r_i = L_i + d_i$ . In this step SB which is part of  $Cr_i$  boundary is updated and after that sub-pixels belonging to the endmember  $i$  are located around  $C_i$  and between pixel margin and calculated SB.

### 3. EXPERIMENTAL RESULTS

The proposed method is compared with SPSAM [8] and the overall accuracy is calculated for classification of the urban area of Pavia University, Italy<sup>3</sup> (See Fig. 2) and the urban area of Kalmthout municipality, Belgium (See Fig.3 3) as ground truths. The ground truths are downsampled by 4 different scaling factors. The method for downsampling is explained as follow:

A window with a size of  $P \times P$  moves over the ground truth. A mixed pixel is created from the pixels of the window. This pixel has different endmembers (all existing classes in the ground truth) with different abundance fractions. Abundance fraction for each endmember is the number of pixels belongs to each class inside the window divided by  $P^2$ . After that window moves and makes another mixed pixel until all the pixels of ground truth are down sampled by this method. This window is a nonoverlap window. When window reaches the

<sup>3</sup>[http://www.ehu.eus/ccwintco/index.php?title=Hyperspectral\\_Remote\\_Sensing\\_Scenes](http://www.ehu.eus/ccwintco/index.php?title=Hyperspectral_Remote_Sensing_Scenes)

**Table 1.** sub-pixel mapping results for Pavia university

	SPSAM		Proposed method	
	$\kappa$	OA%	$\kappa$	OA%
$S = 5$	0.874	95.489	0.892	96.107
$S = 7$	0.799	92.735	0.826	93.714
$S = 9$	0.729	90.398	0.750	91.143
$S = 11$	0.681	88.550	0.702	89.283

**Table 2.** sub-pixel mapping results for Kalmthout area.

	SPSAM		Proposed method	
	$\kappa$	OA%	$\kappa$	OA%
$S = 5$	0.814	95.001	0.857	96.169
$S = 7$	0.732	92.762	0.785	94.189
$S = 9$	0.669	90.974	0.708	92.039
$S = 11$	0.609	89.352	0.649	90.429

final rows or columns and the number of pixels is lower than the number of elements of the window, final row (or column or both, depends on the location of the window) is repeated until the window be filled.

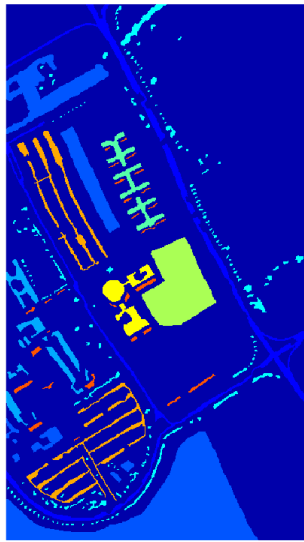
After downsampling, upsampling is done by proposed method and SPSAM. The obtained classification results for proposed algorithm and SPSAM for Pavia University and Kalmthout area datasets in Tables 1 a 2 with different scaling factors. The recontacted ground truths for proposed and SPSAM methods for Pavia University and Kalmthout municipality at scale factor 7 are shown in Figs. ?? and ?? respectively.

#### 4. CONCLUSION

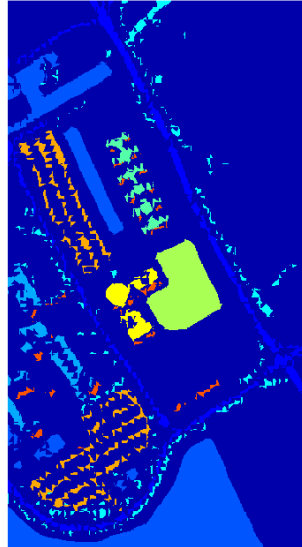
In this paper, a new method for sub-pixel mapping is introduced. This method uses attraction model and by considering a CP and SB between different endmembers. The obtained results show that the efficiency of proposed algorithm. This method can be used to reconstruct the boundaries well, but for reconstruction of lines such as rivers, roads and etc it is not very efficient. In future our aim is to improve the performance of the proposed algorithm.

#### 5. REFERENCES

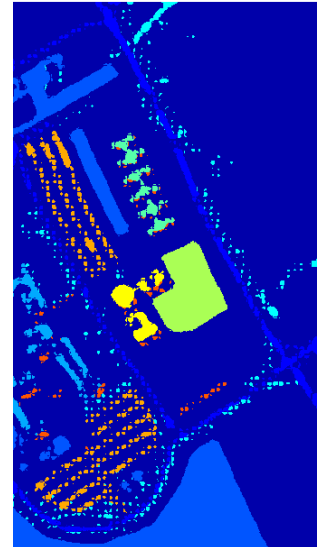
- [1] Zohaib Mahmood, Muhammad Awais Akhter, Guy Thoonen, and Paul Scheunders, "Contextual subpixel mapping of hyperspectral images making use of a high resolution color image," *Selected Topics in Applied Earth Observations and Remote Sensing, IEEE Journal of*, vol. 6, no. 2, pp. 779–791, 2013.
- [2] Zahra Hashemi Nezhad, Azam Karami, Rob Heylen, and Paul Scheunders, "Fusion of hyperspectral and multispectral images using spectral unmixing and sparse coding," .
- [3] Huihui Song, Bo Huang, Kaihua Zhang, and Hankui Zhang, "Spatio-spectral fusion of satellite images based on dictionary-pair learning," *Information Fusion*, vol. 18, pp. 148–160, 2014.
- [4] Jan Verhoeve and Robert De Wulf, "Land cover mapping at sub-pixel scales using linear optimization techniques," *Remote Sensing of Environment*, vol. 79, no. 1, pp. 96–104, 2002.
- [5] Yuan-Fong Su, Giles M Foody, Anuar M Muad, and Ke-Sheng Cheng, "Combining hopfield neural network and contouring methods to enhance super-resolution mapping," *Selected Topics in Applied Earth Observations and Remote Sensing, IEEE Journal of*, vol. 5, no. 5, pp. 1403–1417, 2012.
- [6] Quang Minh Nguyen, Peter M Atkinson, and Hugh G Lewis, "Super-resolution mapping using hopfield neural network with panchromatic imagery," *International journal of remote sensing*, vol. 32, no. 21, pp. 6149–6176, 2011.
- [7] Peter M Atkinson, "Mapping sub-pixel boundaries from remotely sensed images," *Innovations in GIS*, vol. 4, pp. 166–180, 1997.
- [8] Koen C Mertens, Bernard De Baets, Lieven PC Verbeke, and Robert R De Wulf, "A sub-pixel mapping algorithm based on sub-pixel/pixel spatial attraction models," *International Journal of Remote Sensing*, vol. 27, no. 15, pp. 3293–3310, 2006.
- [9] Muhammad Awais Akhter, Zahid Mahmood, and Paul Scheunders, "Hyperspectral image subpixel mapping using getis index," .
- [10] Xiaohua Tong, Xiaobing Zhang, Jerry Shan, Huan Xie, and Minggang Liu, "Attraction-repulsion model-based subpixel mapping of multi-/hyperspectral imagery," *Geoscience and Remote Sensing, IEEE Transactions on*, vol. 51, no. 5, pp. 2799–2814, 2013.



(a) Ground truth image

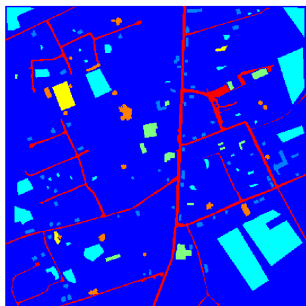


(b) Proposed method at scale 7

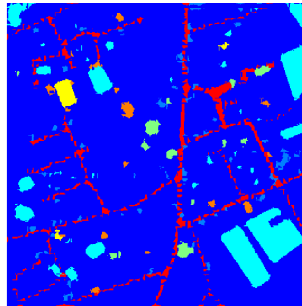


(c) SPSAM at scale 7

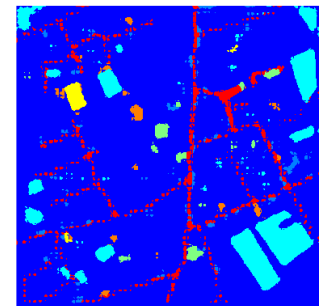
**Fig. 2.** Sub-pixel mapping result of proposed method for urbun area of Pavia University map at different scale factors



(a) Ground truth image



(b) Proposed method at scale 7



(c) SPSAM at scale 7

**Fig. 3.** Sub-pixel mapping result of Kalmthout area at scale factors 7